# Stress in a sweeping arm of a reduction furnace by finite element

# Tensiones en un brazo de barrido de un horno de reducción por elementos finitos

**Daniela García Torres** dgarciat@ismm.edu.cu (1)
**Lisander Romero Breffe** lromerob@ismm.edu.cu (1)
**Keyla Fuentes Cuello** kfuentescoello@gmail.com (1)
(1).University of Moa, Moa, Cuba

**Abstract:** The stresses occurring in a sweep arm made of HK 40 refractory steel used in a reduction furnace were determined through the Finite Element Method. For stress determination, SOLIDWORKS 2020 software was employed, which facilitated geometric and parameterized modeling, meshing of the sweep arm, definition of load cases and their parameters, as well as the model's boundary conditions. Von Mises stress was found to be 1, 313 E 7 $N/m^2$; according to the results obtained, the maximum displacement occurs at a peak value of 8,318 E-1 mm.

**Keywords:** mechanical deformation, numerical method, refractory metal

**Resumen:** Se determinaron las tensiones que se originan en un brazo de barrido de acero refractario HK 40 empleado en un horno de reducción a través del Método de los Elementos Finitos. Para la determinación de las tensiones se empleó el *software* SOLIDWORKS 2020, a través del cual se realizó la modelización geométrica y parametrizada, el mallado del brazo de barrido y la definición de los casos de carga y de sus parámetros, así como las condiciones de frontera del modelo. Se determinó que, la tensión de Von Mises es de 1, 313 E 7 $N/m^2$; según los resultados obtenidos el máxima desplazamiento ocurre a un valor máximo de 8,318 E-1 mm.

**Palabras clave:** deformación mecánica, método numérico, metal refractario

## Introduction

Mathematical simulations of processes have driven an evolution in industry, especially within various engineering branches, as they have enabled the development of industrial

processes with the advantage of cost reduction (Mañay *et al.*, 2022; Izurieta, Buenaño & Rivera, 2024). To carry out simulation, it is important to develop a modeling process and consider input and output variables as well as the environment where the process will unfold (Chariguaman *et al.*, 2022; Elías-González *et al.*, 2024). Simulation can be performed by different methods according to the complexity of the problem to be solved and the required solution.

Finite Element Analysis is an approximate model containing basic variables that allow modification of the prototype, saving time and costs (Márquez *et al.*, 2022; Pérez, 2024; De la Colina, 2024). Currently, computating advances enable the creation of various software tools that perform calculations with finite elements. Knowledge on finite element principles and the materials involved is essential to obtain realistic analyses (González, González & López, 2020; Pozo-Safla, Aquino-Arroba & Ordoñez-Viñan, 2021).

Simulation methodology has become generalized and constitutes a powerful numerical calculation tool capable of solving mathematically, physically, and mechanically formulable problems. It allows simulation and analysis of complex components and structures that are difficult to calculate with traditional analytical methods. Numerical solutions of mathematical equations describing the studied phenomena can be obtained using computers. Therefore, it can be assumed that its accuracy depends on the initial equations and the computers capacity to solve them, hich imposes limitations on its application (Sánchez, 2011).

Huang and Usmani (2012) describe the finite element method as comprising three processes: the Rayleigh-Ritz variational formulation, integration environment overlay with compact intervals interconnected by nodes, and implementation of the weighted residuals algorithm. Specifically, in stress-strain analysis of elements subjected to dynamic loading, the method enables determination of components and deformation states at certain characteristic points. This type of analysis constrains deformation of the study object and localizes highly or lightly stressed zones.

In the 1970s and 1980s, parts modeling was performed via two-dimensional simplified models due to computational limitations at that time. The 2D modeling advantage lies in producing simple models and significantly reducing calculation time, sometimes yielding acceptable results. Hibbitt and Marcal (1973) were pioneers in applying 2D models to determine residual stresses. Despite current computational advances, many

authors still work with 2D planar or axisymmetric models, assuming certain assumptions and simplifications (Lu and Hassan, 2001).

Zhu and Chao (2002) argue that the thermo-deformational response of all mechanical units is three-dimensional and only such models can fully reproduce the phenomenon in real static analyses. This modeling has been applied by various authors (Lu and Hassan, 2001; Vinas *et al.*, 2005). Lu and Hassan (2001) simulated a static four-pass analysis using a 3D model, reporting tensile and compressive residual stress concentrations at the start and end points that 2D models cannot capture.

Reduction furnaces for lateritic ores have, in the sweep mechanism, arms manufactured through casting (Correa-Suárez, Rodríguez-González & Pompa-Larrazabal, 2020). To manufacture sweep arms for nickel industry reduction furnaces, HK-40 refractory steel is used (Fernández Columbié *et al*., 2023). According to Fernández Columbié, Suárez Torres & Rodríguez González (2024), when refractory steel is subjected to tensile stresses, small cavities form in its microstructure during high-temperature operation.

The aim of this study is to determine the stresses arising in a sweep arm, made of HK 40 refractory steel, used in a reduction furnace through the Finite Element Method.

## Materials and Methods

### Finite Element Stress Modeling

Upon obtaining the structural analysis file (Figure 1), it is executed via static equilibrium analysis, wherein nodal stresses, at each course of time generated by the run, are read and applied as nodal loads in the structural run. Thus, each static structural analysis starts from the final deformation and stress state of the previously concluded analysis. This is valid since plastic deformations are irreversible regardless time (if viscoplastic deformation at high temperatures is neglected), so time integration is unnecessary for this analysis.

This analysis was mainly performed in programming mode.

The analysis type declared was the static.

Full Newton-Raphson iterative method for nonlinear differential equations solution used was, which constitutes the SOLIDWORKS standard nonlinear method for plasticity problems.

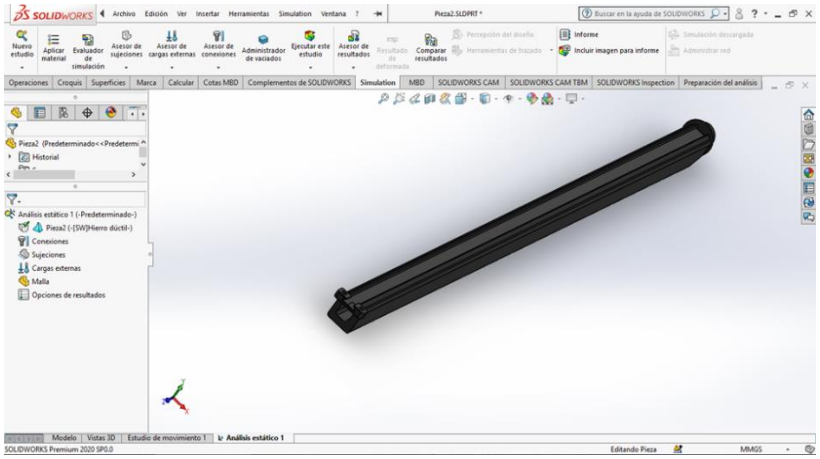

Figure 1. Model simulation.

Meshing is a crucial step in design analysis, as it is a primary factor upon which the final results depend. Initially, the software estimates a global element size for the model taking into account its volume, surface area, and geometric details. The mesh size generated (number of nodes and elements) depended on model geometry and dimensions, element size, tolerance, mesh control, and contact specifications. Figure 2 corresponds to the meshing.

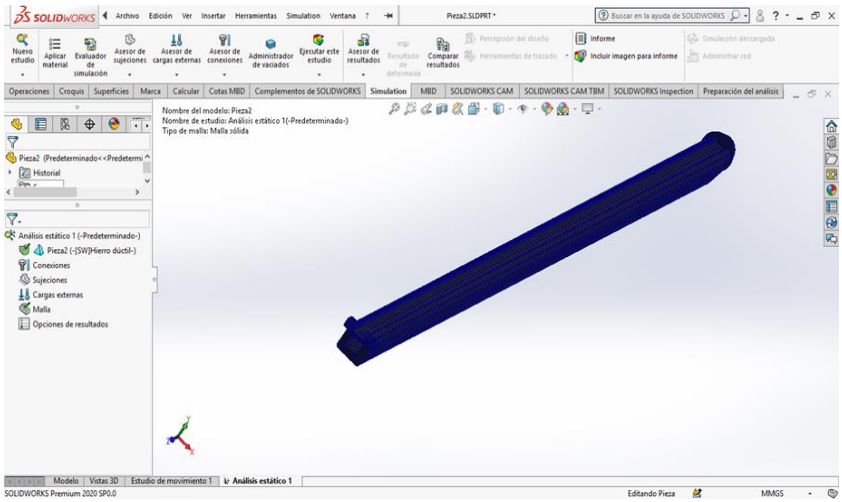

Figure 2. Model meshing.

The software allows finer meshing in areas of interest, in other words, where stresses are higher, enabling increased definition and detail. Using a mesh with these characteristics does not affect result accuracy but saves time and memory during simulation execution.

Boundary conditions (figure 3) were set to avoid rigid body motion and to estimate deformation and stress states produced by external loads applied to the system by restricting part of the domain (u = 0 for domain Su). In this case, applied forces were treated as distributed loads over small but finite areas. These conditions were defined in the ST domain.

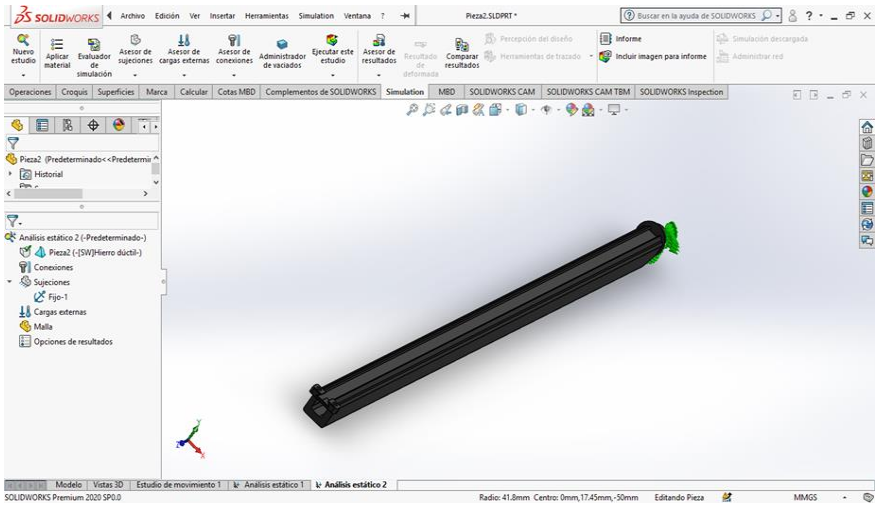


Figure 3. Boundary conditions.

Under these boundary conditions, the threshold torque is defined as the borderline value between the model´s elastic and plastic regimes. The way contiguous elements will be connected (through a rigid node or allowing some relative deformation) was determined, along with their respective mount conditions (embedding, articulation, or simple mount).

For a model with imposed actions, those affecting the structure for a given operating condition were established (Figure 4), represented by sets of loads or imposed deformations, both internal and external, occurring on the sweep arm under stress and deformation states.

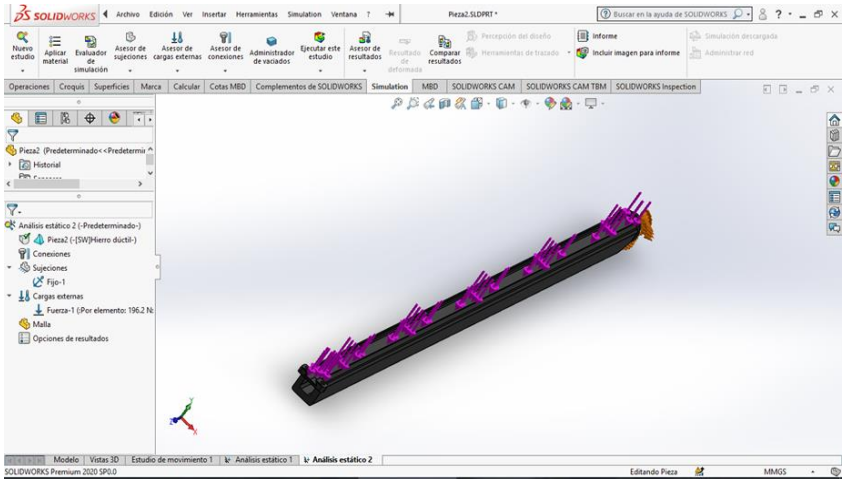

Figure 4. Load assignment to the model.

For load assignment, the body was considered three-dimensional, subjected to loads and pressures, where any point is defined by coordinates x, y, z. The surface or boundary is constrained to a region where displacement is specified. A force is introduced and locked in successive loading steps so that effects initially produced by the force are preserved as displacements after locked.

This procedure was used considering that collapse forces and different failure modes can thereby be reproduced. It is also possible to obtain stresses, strains, and displacements at desired points to create force-displacement or stress-strain curves similar to the ones obtained in real tests.

## Results and Discussion

### Finite Element Method Analysis

One way to characterize steel´s plastic properties is through Johnson-Cook mechanical model, which replicates material behavior under large strains, high temperatures, and high strain rates. This model's formulation defines Von Mises equivalent stress as three decoupled terms: the first, defines strain hardening dependence; the second, strain sensitivity; and the third, temperature sensitivity. Figure 5 shows the analysis of stresses the sweep arm is subjected to.

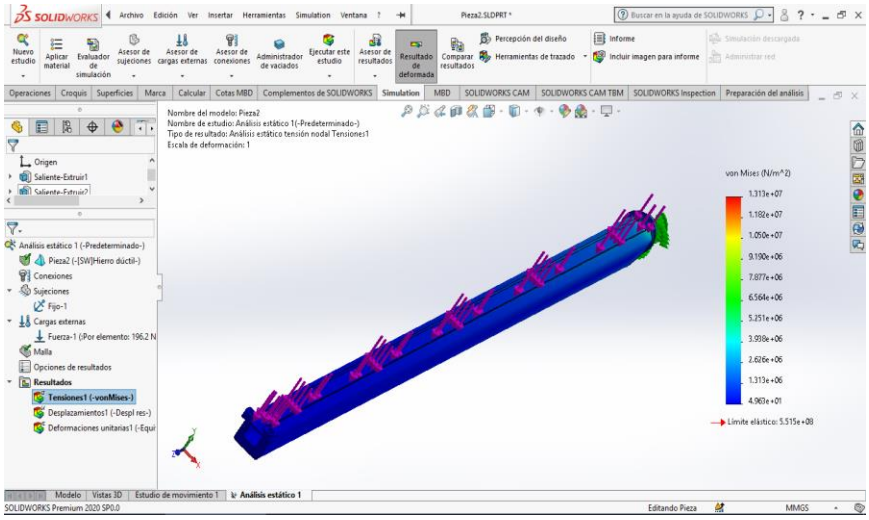


Figure 5. Von Mises maximum equivalent stress.

In this scenario, the arm operates under rigid conditions, and it can be observed that, the Von Mises stress distribution shows that the most critical areas appear to be theoretical. It is determined that the maximum stress in the sweep arm is 1.313 E 7 N/m².

The use of elastic stress concentration factors indicates the average load required on a part to cause plastic deformation or creep; these factors are also useful to analyze loads in a part that could cause fatigue fracture. Displacements to which the sweep arm of the reduction furnace is exposed were determined; this behavior is shown in Figure 6.

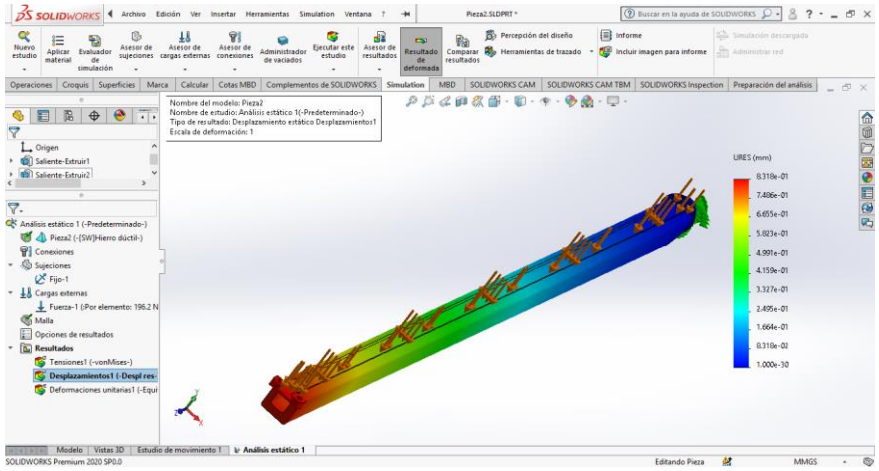


Figure 6. Displacement behavior.

Displacements exhibit symmetric behavior along the vertical axis. The maximum displacement occurs at a peak value of 8,318 E-1 mm; this occurs at the sweep arm's end, where the highest stress concentration (red zone) exists and where failure is thus

most likely to happen. While one end of the sweep arm is exposed to deformation processes, the other end, embedded into the furnace base, is under compression conditions (blue zone).

Regardless of parameters analyzed to determine total deformation effect on the sweep arm (modulus of elasticity and Poisson's ratio), there are other parameters that influence this deformation state during furnace operation, including temperature effect. If temperature rises above the original value, the associated deformation can be considered. For isotropic materials, the increase of this factor results in uniform deformation depending on the element's linear expansion coefficient, which is assumed as a constant within the variation range. Deformation due to this temperature change causes no stress when the body is free to deform, as explained by Srivastava *et al.* (2015).

## Conclusions

Stresses occurring in a sweep arm made of HK 40 refractory steel used in a reduction furnace were determined via the Finite Element Method.

It was determined that stresses in the sweep arm can be influenced by various factors such as arm geometry, applied load, and material properties.

The Von Mises maximum equivalent stress to which the reduction furnace sweep arm is subjected is 1, 313 E 7 $N/m^2$, indicating the component undergoes significant loads and may be at risk of fracture failure.

## Bibliographic References

Correa-Suárez, R.E., Rodríguez-González, I. & Pompa-Larrazabal, M. (2020). Diseño de herramienta para mecanizado de brazos de hornos de soleras múltiples. *Ciencias Holguín*, 26(2), 71-81. https://www.redalyc.org/articulo.oa?id=181563169006

Chariguaman, L. S. C., Arroba, S. M. A., Pérez, L. P. T. & Robles, C. E. M. (2022). Estudio de metodologías para la modelación matemática y simulación de engranes rectos para validar su diseño. *Polo del Conocimiento*, *7*(7), 2380-2402. https://dialnet.unirioja.es/servlet/articulo?codigo=9042954

De la Colina Martínez, J. (2024). Métodos analíticos y numéricos para el análisis de placas delgadas. *Ideas en Ciencias de la Ingeniería*, *2*(3), 89-104. https://ideasencienciasingenieria.uaemex.mx/article/view/24425

Elías-González, J. E., Salazar-Álvarez, É. G., Orozco, D. Y., Guerrero, E. C., Vera, D. Z., Robles, C. E. M. & Ujukam, T. J. E. (2024). Modelación y simulación computacional de una trituradora de biomasa forestal en Ecuador. *TecnoLógicas*, *27*(61). https://revistas.itm.edu.co/index.php/tecnologicas/article/view/3244

Fernández Columbié, T., Suárez Torres, L., Rodríguez González, I., Guzmán Romero, E.E., Caraballo Núñez, M.A. (2023). Efecto de la temperatura de termofluencia en el acero austenítico refractario HK-40. *Ingeniería Mecánica*, 26(1). http://scielo.sld.cu/scielo.php?script=sci_isoref&pid=S1815-59442023000100060&Ing=es&tIng=en

Fernández Columbié, T., Suárez Torres, L., Rodríguez González, I. (2024). Determinación de los componentes metalúrgicos de la aleación HK 40 empleada en dientes de barrido luego del proceso de fundición. *Ingeniería Mecánica*, 27(1), 354-42. http://scielo.sld.cu/scielo.php?pid=S1815-59442024000100035&script=sci_arttext

González Woge, O., González Morán, C. O. & López Chau, A. (2020). Introducción al método del elemento finito: Solidworks y Matlab. *Ideas en Ciencias de la Ingeniería*, 1(1), 27-47. https://ideasencienciasingenieria.uaemex.mx/article/view/14589

Hibbitt, H. & Marcal, P. (1973). A numerical thermo-mechanical model of the welding and subsequent loading of a fabricated structure. *Computadoras y estructuras,* 3(5), 1145-1174. https://doi.org/10.1016/0045-7949(73)90043-6

Huang, H. & Usmani, A. (2012). *Finite element analysis for heat transfer*. Springer Science & Business Media.

Izurieta, C., Buenaño, S. & Rivera, M. (2024). El diseño industrial y la simulación como herramienta para mejorar los procesos. *Polo del Conocimiento*, *9*(3), 695-706. https://www.polodelconocimiento.com/ojs/index.php/es/article/view/6674

Lu, X. & Hassan, T. (2001). Tensiones residuales en uniones soldadas a tope y a encaje. *Transactions,* 16, 1-8 https://repository.lib.ncsu.edu/server/api/core/bitstreams/034c9c28-0775-4171-ae54-3309d7f9fea8

Mañay, E. D., Chiliquinga, M. D., Ugsha, H. E. Y. & Castillo, P. S. (2022). Diseño por simulación de un control Fuzzy y MPC para un proceso de nivel. *Ciencia Latina*, *6*(1), 1951-1970. https://www.ciencialatina.org/index.php/cienciala/article/view/1621

Márquez, J. A. S., Ramírez, T. A. S., González, A. G., Jiménez, L. S. M., Guía, K. N. N., Rodríguez, M. R., & Ramírez, F. M. S. (2022). Simulación del Esfuerzo Mecánico en una pieza Modelada en 3D por el Método de Elementos Finitos. *Jóvenes en la ciencia*, *16*, 1-10. https://www.jovenesenlaciencia.ugto.mx/index.php/jovenesenlaciencia/article/view/3567

Pérez, J. I. (2024). Verificación de los estados límite últimos por métodos numéricos en el marco de la segunda generación del Eurocódigo7. *Revista Digital del Cedex*, (204), 61-76. https://ingenieriacivil.cedex.es/index.php/ingenieria-civil/article/view/2506

Pozo-Safla, E. R., Aquino-Arroba, S. M. & Ordoñez-Viñan, M. A. (2021). Análisis estadístico para validar la simulación por elemento finito en el diseño a deformación de una viga en voladizo. *Polo del Conocimiento*, *6*(6), 586-611. https://www.polodelconocimiento.com/ojs/index.php/es/article/view/2771

Sánchez, D. (2011). *Análisis de tensiones en piezas mecánicas de geometría cilíndrica utilizando el método de los elementos finitos*. (Trabajo de Diploma, Universidad de Salamanca, España). https://gredos.usal.es/handle/10366/120402

Srivastava, A., Ponson, L., Osovski, S., Bouchaud, E., Tvrgaard, V., Ravi Chandar, K. & Needleman, A. (2015). The effect of loading rate on ductile fracture toughness and fracture surface roughness. *Journal of Mechanics and Physics of Solids*, 76(7), 20-46. https://doi.org/10.1016/j.jmps.2014.11.007

Vinas, G., Dauda, T. & Moyes, N. (2005). Finite element analysis of residual stresses in a setter box excavation repair weld for Chapel cross Power Station. *International Journal of Pressure Vessels and Piping,* 82(11), 270-278. https://doi.org/10.1016/j.ijpvp.2004.08.005

Zagal, K. C., Bustamante, D. B. V. & Cuasapaz, D. P. G. (2023). Comportamiento estructural de cubiertas tipo tenso membranas empleando el método de elementos finitos. *Green World Journal*, *6*(6), 1-21. https://pure.ups.edu.ec/es/publications/structural-behavior-of-tensile-membrane-roofs-*using-the-finite-el*

Zhu, X. & Chao, Y. (2002). Effects of temperature dependent material properties on welding simulation. *Computers and Structures*, 80(11), 967-976. https://doi.org/10.1016/S0045-7949(02)00040-8